

Numerical study of the critical behavior of the Ashkin-Teller model at a line defect

Péter Lajkó^{1,*} and Ferenc Iglói^{2,3,†}

¹*Department of Physics, Kuwait University, P.O. Box 5969, Safat 13060, Kuwait*

²*Research Institute for Solid State Physics and Optics, H-1525 Budapest, P.O.Box 49, Hungary*

³*Institute of Theoretical Physics, Szeged University, H-6720 Szeged, Hungary*

(Dated: January 20, 2013)

We consider the Ashkin-Teller model on the square lattice, which is represented by two Ising models (σ and τ) having a four-spin coupling of strength, ϵ , between them. We introduce an asymmetric defect line in the system along which the couplings in the σ Ising model are modified. In the Hamiltonian version of the model we study the scaling behavior of the critical magnetization at the defect, both for σ and for τ spins by density matrix renormalization. For $\epsilon > 0$ we observe identical scaling for σ and τ spins, whereas for $\epsilon < 0$ one model becomes locally ordered and the other locally disordered. This is different of the critical behavior of the uncoupled model ($\epsilon = 0$) and is in contradiction with the results of recent field-theoretical calculations.

I. INTRODUCTION

In a system which is divided into two parts by a defect plane translational invariance is broken and the physical properties are different in the defect region, which has a width of the correlation length, ξ . At the critical point where ξ is divergent the scaling properties of local quantities, such as the defect magnetization or the spin-spin correlation function, could be different from that in the bulk[1]. Relevance or irrelevance of the perturbation caused by a weak defect can be analyzed within the frame of phenomenological scaling theory[2–5]. If the perturbation is coupled to the local energy operator, then the bulk fixed point is stable if the correlation length critical exponent of the pure system, ν , is greater than 1. In this case the defect exponents are the same as at any other point of the bulk. In the opposite case for $\nu < 1$, generally a new fixed point governs the local critical behavior, the properties of which are different for weakened and for enhanced local couplings. For weakened defect couplings the defect usually renormalizes to a cut and the local critical behavior is the same as at the ordinary surface critical point[6–8]. On the contrary for enhanced defect couplings the defect usually renormalizes to an ordered interface and the local critical exponents are the same as at the extraordinary surface transition[6–8]. Examples for modified defect critical behavior can be found in the two-dimensional (2D) $q = 3$ state Potts model[9, 10], in the Baxter-Wu model[11] or in the Ashkin-Teller (AT) model[12].

According to scaling considerations in a system having a correlation length exponent $\nu = 1$ a defect is a marginal perturbation. This happens for the 2D Ising model for which the local magnetization[13] and the spin-spin correlation function at the defect[14] has been exactly calculated and the local critical exponent of the magnetization is found to be a continuous function of the strength of the

defect. These results have been generalized recently for inhomogeneous line defects, in which the defect coupling is a smooth function of the position[15].

In a system which has more complicated interaction between the spin variables one can define special defects which influence only some parts of the interaction. This type of asymmetric defect has been considered recently by Naon[16] in the AT[17] and in the Baxter models[18]. We remind that both the AT and the Baxter models are expressed in terms of two sets of Ising spin variables[19], say σ and τ , with two-site (K_2) and four-site (K_4) interactions. The asymmetric defect introduced by Naon is represented by a line of modified two-spin couplings in one of the Ising models (say for the σ spins), whereas the other interactions are left unchanged. Using field-theoretical methods Naon has determined the decay of the critical spin-spin correlation function, both for the σ and for the τ spins and the calculated local magnetization exponents are found to be independent of the interaction between the Ising models, which is measured by $\epsilon = K_4/K_2$. Similar results are obtained in the case of an asymmetric and inhomogeneous line defect in the AT model[15]. These results are somewhat surprising, since in the pure AT and Baxter models ϵ is a marginal perturbation and several (bulk and surface) critical exponents are continuous functions[20] of ϵ .

In this paper we are going to revisit this type of problem and study numerically the local critical behavior at an asymmetric defect in the AT model. Our aim is to shed some light to the physical mechanism which is behind this problem and to confront the measured critical exponents with the results of field-theoretical calculations. Here we shall consider both chain and ladder type defects[1] and the system is studied by the transfer matrix, which is perpendicular to the defect. We use the Hamiltonian limit[21, 22] of the transfer matrix and calculate the local magnetization both for σ and τ spins by density matrix renormalization[23] (DMRG). At the critical point the local magnetization exponents are then deduced through finite-size scaling.

The structure of the paper is the following. The model and its basic properties are described in Sec. II. Numer-

*Electronic address: peter.lajko@ku.edu.kw

†Electronic address: igloi@szfki.hu

ical results of the scaling of the interface magnetization are presented in Sec. III and discussed in Sec. IV.

II. THE AT MODEL WITH A DEFECT LINE

The AT model is defined in terms of a four-state spin variable[17], which is represented by a pair of Ising spins: $\sigma_i = \pm 1$ and $\tau_i = \pm 1$ at the lattice site i . Between the same set of spins there is nearest neighbor interaction of strength K_2 and the two Ising models are coupled by the product of the energy densities, which is given by a four-spin term: $K_4\sigma_i\sigma_j\tau_i\tau_j$, where i and j are nearest neighbors. We consider the system on the square lattice and work with the row-to-row transfer matrix \mathcal{T}_{AT} . In the Hamiltonian limit the transfer matrix can be written as $\mathcal{T}_{AT} \sim \exp(-\kappa\mathcal{H}_{AT})$, where κ is the lattice spacing in the “time” direction and \mathcal{H}_{AT} is a one-dimensional quantum Hamiltonian given by[21, 22]

$$\mathcal{H}_{AT} = - \sum_i (\sigma_i^z \sigma_{i+1}^z + \tau_i^z \tau_{i+1}^z) - h \sum_i (\sigma_i^x + \tau_i^x) - \epsilon \left[\sum_i \sigma_i^z \sigma_{i+1}^z \tau_i^z \tau_{i+1}^z + h \sum_i \sigma_i^x \tau_i^x \right]. \quad (1)$$

Here $\sigma_i^{x,z}$ and $\tau_i^{x,z}$ are two sets of Pauli matrices at site i and h is the strength of the transverse field, which plays the role of the temperature in the classical system. As before the ratio of the couplings is denoted by $\epsilon = K_4/K_2$.

The system in Eq.(1) is self-dual and the self-duality line: $h_c = 1$ represents the critical line separating the ferromagnetic and the paramagnetic phases of the system for $-1/\sqrt{2} \leq \epsilon \leq 1$. In the region $-1 < \epsilon \leq -1/\sqrt{2}$, there is a so-called “critical fan”, which extends to both sides of the self-duality line and in which the system stays critical [21].

The critical properties of the AT model are exactly known through conformal invariance and Coulomb-gas mapping [24, 25]. The decay of the spin-spin correlations:

$$\langle 0 | \sigma_i^z \sigma_{i+r}^z | 0 \rangle = \langle 0 | \tau_i^z \tau_{i+r}^z | 0 \rangle \sim r^{-2x_m} \quad (2)$$

is characterized by the anomalous dimension, $x_m = 1/8$, which does not depend on the value of the coupling ϵ . On the contrary the decay of the connected energy-energy correlations:

$$\langle 0 | \sigma_i^x \sigma_{i+r}^x | 0 \rangle - \langle 0 | \sigma_i^x | 0 \rangle \langle 0 | \sigma_{i+r}^x | 0 \rangle \sim r^{-2x_e} \quad (3)$$

involves the anomalous dimension: $x_e = \pi/[2 \arccos(-\epsilon)]$, which is ϵ dependent[21]. Similar holds for the correlation length critical exponent ν , which is given by: $\nu = 1/(2 - x_e)$ for $-1/\sqrt{2} \leq \epsilon \leq 1$ whereas it is formally infinite in the critical fan.

Finally, the decay of the end-to-end correlation function at the critical point involves the surface magnetization scaling dimension, x_m^s :

$$\langle 0 | \sigma_{-L}^z \sigma_L^z | 0 \rangle = \langle 0 | \tau_{-L}^z \tau_L^z | 0 \rangle \sim L^{-2x_m^s} \quad (4)$$

which is also coupling dependent[26]: $x_m^s = \arccos(-\epsilon)/\pi$.

The marginal operator for the AT model is associated with the four-spin term, $\sigma_i^z \sigma_{i+1}^z \tau_i^z \tau_{i+1}^z$, which has a scaling dimension, $x_4 = 2 = D$, independently of ϵ , for $-1 \leq \epsilon \leq 1$.

A. Ladder and chain defects

A line defect in the 2D classical model is put in the “time” direction and can be of two types: chain defect or ladder defect (see Fig. 6.1 of Ref. [1]). In the problem studied by Naon[16] and we consider here a line of two-spin couplings between the σ -spins are modified. In the Hamiltonian limit, when the defect is placed between sites $i = 0$ and $i = 1$ (ladder defect) the perturbation is given by:

$$\mathcal{V}_{\text{ladder}} = -(J - 1)\sigma_0^z \sigma_1^z, \quad (5)$$

where J is the strength of the defect. On the other hand for a chain defect with modified two-spin couplings at line $i = 0$ the perturbation in the Hamiltonian limit involves the term:

$$\mathcal{V}_{\text{chain}} = -(\tilde{h} - h)\sigma_0^x. \quad (6)$$

The ladder and chain defects transforms into each other through duality[12] and their strengths are related as: $\tilde{h} \leftrightarrow 1/J$.

For two decoupled Ising models with $\epsilon = 0$ the local magnetization exponents at the defect site, $i = 0$, generally are different for the σ and for the τ spins, which are denoted by x_m^σ and x_m^τ , respectively. While x_m^τ keeps its bulk value, x_m^σ is a continuous function of the strength of the defect[13, 14]:

$$x_m^\sigma(J) = \frac{2}{\pi^2} \arctan^2(1/J), \quad x_m^\tau = 1/8, \quad \epsilon = 0, \quad (7)$$

for a ladder defect and

$$x_m^\sigma(\tilde{h}) = \frac{2}{\pi^2} \arctan^2(\tilde{h}), \quad x_m^\tau = 1/8, \quad \epsilon = 0, \quad (8)$$

for a chain defect. For σ spins the marginal operator is the local energy density, which has its anomalous dimension $x_e = 1$, independently of the value of J or \tilde{h} .

If we switch on the interaction between the Ising models the defect critical behavior could be modified. For small ϵ the anomalous dimension of the four-spin operator is $x_4 = x_e^\sigma + x_e^\tau = 2$, which is just the marginal value. We note, however, that field-theoretical calculations of the critical spin-spin correlation function[16] come to the conclusion, that ϵ is an irrelevant variable. Here we revisit this problem by numerical methods.

III. NUMERICAL STUDY

Here we consider the Hamiltonian version of the AT model at a finite lattice with $-L \leq i \leq L$ and use fixed-spin boundary conditions: $\sigma_{\pm L}^z = \tau_{\pm L}^z = +1$. Using the DMRG method we calculate the ground-state expectation value of the magnetization operators at the defect, $\langle 0 | \sigma_0^x | 0 \rangle = m_0^\sigma(L)$ and $\langle 0 | \tau_0^x | 0 \rangle = m_0^\tau(L)$. The parameters in Eq.(1) are taken at different points of the critical line: $h = h_c = 1$ and $-1 < \epsilon \leq 1$ and we have considered different strengths of the defect: $\tilde{h} > 0$ and $J > 0$. According to finite-size scaling theory these magnetizations asymptotically behave as:

$$m_0^\alpha(L) \sim L^{-x_m^\alpha}, \quad \alpha = \sigma, \tau. \quad (9)$$

In the numerical calculation we went up to $L = 85$ and in the DMRG method we have generally kept around $m = 150$ states of the density matrix in order to obtain a good numerical accuracy.

From the values of the matrix element in Eq.(9) at two different sizes, L and bL , we have calculated effective, size-dependent exponents through two-point fits:

$$\frac{\ln m_0^\alpha(bL) - \ln m_0^\alpha(L)}{\ln b} = x_m^\alpha(L). \quad (10)$$

In order to obtain the same numerical accuracy for the different lengths, we keep the ratio b between neighboring sizes approximately constant. The effective exponents evolve towards their exact values when the mean size associated with the two-point fit, $\langle L \rangle = L(b+1)/2$, tends to infinity.

In the actual calculation we consider first in Sec.III A the known limiting cases (decoupling limit, system without defect) in order to check the accuracy of the numerical method. Afterward we study the general model with defect for $\epsilon > 0$ and $\epsilon < 0$ in Sec.III B and in Sec.III C, respectively.

The numerical calculations are performed on several PC-s, the total CPU time being equivalent to ~ 250 days in a single 2.4 GHz processor. We note that an alternative numerical method is to use Monte Carlo (MC) simulations on the classical model with $L \times M$ sites. As can be seen in an investigation of a related problem[27] the DMRG and the MC methods generally provide results with approximately the same accuracy using the same CPU times.

A. Decoupled or non-defected systems

We start with the decoupled model and calculate the critical local magnetization of the σ Ising model having a ladder defect. The finite-size magnetization exponents, $x_m^\sigma(L)$, which have been obtained through Eq.(10) are plotted as a function of $1/L$ in the left panel of Fig.1 for different strength of the defect, J . Extrapolating for large L the limiting exponents are in good agreement

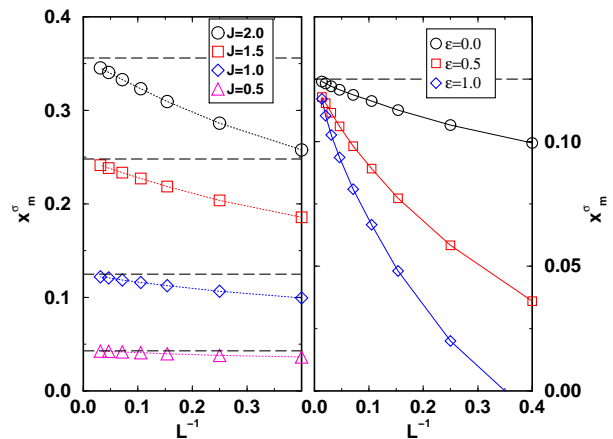


FIG. 1: Numerical estimates of the magnetization exponent $x_m^\sigma(L)$ for different finite systems of length L at special points of the phase diagram. Left panel: at the decoupling point, $\epsilon = 0$, for various values of the strength of the ladder defect, J . Right panel: non-defected AT model for different values of the coupling, ϵ . The exact results are indicated by horizontal broken lines.

with the analytical results in Eq.(7), which are indicated by dashed lines.

We have also studied the AT model without defects, but for different values of the coupling, $\epsilon \geq 0$. The finite-size magnetization exponents, which in this case correspond to the bulk exponents, are plotted as a function of $1/L$ in the right panel of Fig.1. As seen in the figure the extrapolated exponents are fairly close to the exact value, $x_m = 1/8$, which indeed does not depend on ϵ . The correction terms, however, are larger for a more strongly coupled system.

B. Positive coupling: $\epsilon > 0$

This part of the phase diagram of the Hamiltonian model corresponds to the classical model with positive Boltzmann-weights, thus the results obtained in this domain should be compared with the field-theoretical calculations in Ref.[16]. First we present in Fig.2 the finite-size magnetization exponents (both for σ and τ spins) which are calculated at the largest length, $L = 85$. Here we have a system with a chain defect of strength, $\tilde{h} = 1/2, 2/3, 3/4, 1., 4/3, 3/2$ and 2 and various positive values of the coupling. For the sake of comparison we also present the analytical results in the decoupling limit, $\epsilon = 0$, which are plotted with dotted-dashed and broken lines for σ and τ spins, respectively. We note that according to field-theoretical investigations[16] these results should hold for $\epsilon > 0$, too. The numerical results in Fig.2 seem to be in contradiction with the field-theoretical conjectures in two respects. i) The effective (L -dependent) magnetization exponents vary with the coupling, $\epsilon > 0$,

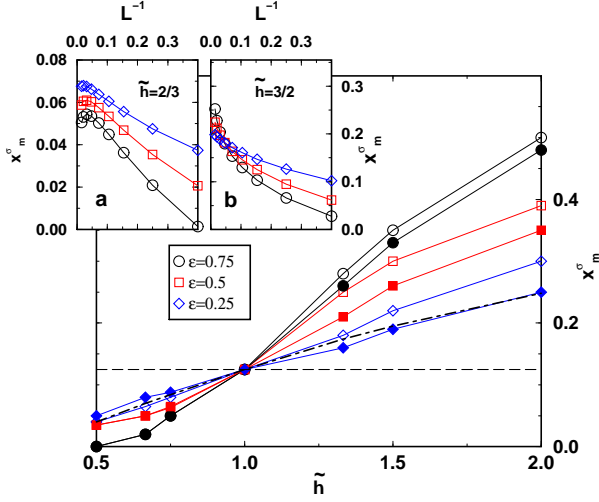


FIG. 2: Finite-size magnetization exponents $x_m^\alpha(L)$ calculated at the largest length L at a chain defect of strength \tilde{h} and for positive values of the coupling, $\epsilon > 0$. The open (filled) symbols are for $\alpha = \sigma$ ($\alpha = \tau$) spins. Note, the very similar scaling behavior of σ and τ spins. The exact results for the decoupled model with $\epsilon = 0$ are indicated by dotted and broken lines, for σ and τ spins, respectively. These represent the field-theoretical result[16]. Insets: Size-dependence of the effective magnetization exponents for σ spins. a) For enhanced defect strength, $\tilde{h} = 2/3$, the finite-size exponents are expected to approach $x_m^\sigma(L) = 0$, which corresponds to an EI fixed point. b) For reduced defect strength, $\tilde{h} = 3/2$, the finite-size exponents are expected to approach $x_m^\sigma = x_m^\tau = x_m^s$, which corresponds to an OI fixed point.

in particular for large ϵ there is a considerable difference from the value at $\epsilon = 0$. ii) The magnetization exponents at the τ spins are different from the predicted bulk value, $x_m = 1/8$, and these are close to that measured values at σ spins at the same system. The trend of the effective exponents with the size of the system is different for enhanced ($J > 1$ or $\tilde{h} < 1$) and reduced ($J < 1$ or $\tilde{h} > 1$) defect couplings, respectively.

For enhanced defect couplings the local magnetization exponents are smaller than the values at the decoupling limit and the finite-size exponents - for sufficiently large sizes - are decreasing with L . This is illustrated in the inset a) of Fig.2 for $\tilde{h} = 2/3$. We expect that this decreasing tendency will continue for larger sizes and the extrapolated exponents will approach $x_m^\sigma = x_m^\tau = 0$. This type of behavior is characteristic for an ordered defect (see Eqs.(7) and (8) for $J \rightarrow \infty$ and $\tilde{h} \rightarrow 0$, respectively), and we assume that the local transition for enhanced couplings is governed by an extraordinary interface (EI) fixed point.

For reduced defect couplings the effective, L -dependent exponents are larger than their value at the decoupling point and these are continuously increasing with L . In order to check a possible overshooting

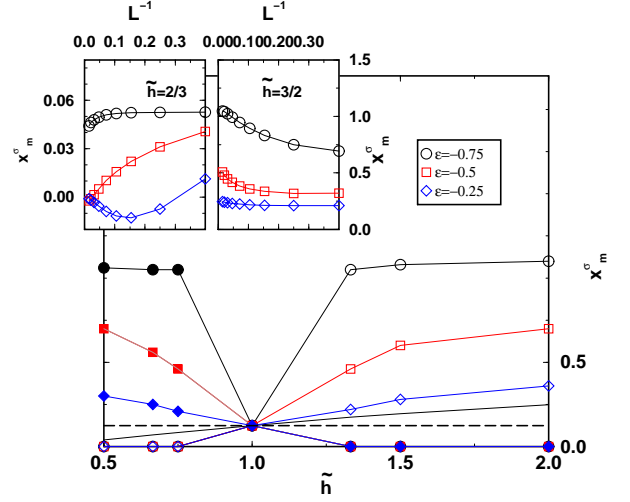


FIG. 3: The same as in Fig.2 but for negative coupling, $\epsilon < 0$. Note, the complementary scaling behavior of σ and τ spins: $x_m^\sigma(\tilde{h}) \approx x_m^\tau(1/\tilde{h})$. Insets: Size-dependence of the effective magnetization exponents for σ spins. a) For enhanced defect strength, $\tilde{h} = 2/3$, the finite-size exponents are expected to approach $x_m^\sigma(L) = 0$, which corresponds to an EI fixed point. b) For reduced defect strength, $\tilde{h} = 3/2$, the finite-size exponents are expected to approach a non-trivial value: $x_m^\sigma(\epsilon)$, which corresponds to a special OI fixed point.

effect we have made calculations up to $L \sim 500$, but no bending of the curves are found. We have also compared the magnetization exponents at the two sublattices, i.e. x_m^σ with x_m^τ . For a finite L , $x_m^\sigma(L)$ is larger than $x_m^\tau(L)$, however the limiting value of the two exponents are very close to each other, see Fig.2 for $\tilde{h} > 1$. We expect, that for the true exponents we have $x_m^\sigma = x_m^\tau$. A more difficult point is to decide about the eventual \tilde{h} -dependence of the exponents. Here one should note that the effective exponents show a quite strong \tilde{h} , as well as L -dependence. As illustrated in the inset b) of Fig.2 the extrapolation of the data with L is very difficult, at least for not too large values of \tilde{h} . To interpret the data we use the hypothesis, that the interface critical behavior is controlled by an ordinary interface (OI) fixed point. In this scenario the true exponents are independent of \tilde{h} and their values are the same as at a free surface, as given below Eq.(4). Indeed, for larger values of \tilde{h} the extrapolated exponents are fairly close to $x_m^s(\epsilon)$.

C. Negative coupling: $\epsilon < 0$

This part of the phase diagram of the Hamiltonian model corresponds to the classical model with negative Boltzmann-weights. The calculated finite-size magnetization exponents for the same absolute values of ϵ and for the same values of \tilde{h} as in Sec.III B are shown in Fig.3.

The two figures, Fig.3 and Fig.2, show several differences. The most important difference is that here the limiting values of x_m^σ and x_m^τ are different. The effective exponents for σ spins with \tilde{h} are approximately equal to the effective exponents for τ spins, however at $1/\tilde{h}$. As far as the defect exponents on the σ spins are concerned the trend is similar as for $\epsilon > 0$. For enhanced defect couplings the finite-size exponents seem to approach $x_m^\sigma = 0$, thus the σ spins are locally ordered and their critical behavior at the defect is controlled by the EI fixed point. On the contrary for reduced couplings at the defect the finite-size exponents are monotonously increasing with the size and they seem to approach a non-trivial value: $x_m^\sigma = x_{\text{def}}(\epsilon)$. We expect, that this limiting value depends only on ϵ , but does not depend on $J < 1$ or $\tilde{h} > 1$, thus it can be identified as a special interface exponent in the model with a vanishing bond, $J = 0$.

IV. DISCUSSION

The numerical results presented in the previous Section about the interface critical behavior of the AT model with a (asymmetric) line defect can be interpreted in terms of an RG phase diagram, which is shown in the right panel of Fig.4 both for the σ and the τ spins. As a comparison in the left panel of Fig.4 we show the RG phase diagram for such a (symmetric) defect, which is proportional with the local energy density and given by:

$$\tilde{\mathcal{V}}_{\text{chain}} = -(\tilde{h} - h)(\sigma_0^x + \tau_0^x + \epsilon \sigma_0^x \tau_0^x), \quad (11)$$

for a chain defect and similarly for a ladder defect. In this case the σ and τ spins play equivalent role and the interface critical behavior has been studied previously in Refs.[11, 12]. According to these results, which are in agreement with a relevance-irrelevance analysis[2–5], the bulk fixed point (B) in the system is unstable for $\epsilon > 0$. The numerical results also indicate that the critical behavior at the defect is governed by the OI and EI fixed points, for reduced and enhanced strength of the defect, respectively. This type of RG phase diagram is suggested to be valid for the asymmetric defect too, as illustrated in the right panel of Fig.4. This result indicate, that the phase-diagram in the left panel of Fig.4 for $\epsilon > 0$ is probably valid in a coarse-grained description: the direction of the flow at B depends only on the condition, if the local energy at the defect is reduced or enhanced with respect to the pure system.

For negative coupling, $\epsilon < 0$, the structure of the phase-diagrams are changed, both for symmetric and asymmetric defects. For symmetric defects the bulk fixed-point becomes the stable one[11, 12]. It is certainly understandable, that the EI fixed point is unstable, since for $\epsilon < 0$ ordered defects would bring a positive contribution to the energy. The same reasoning holds for the

asymmetric defect, too. Thus for $\epsilon < 0$ the σ and the τ spins can not be ordered at the same time. In this case

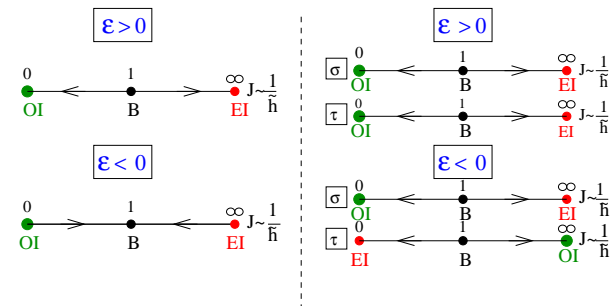


FIG. 4: Schematic RG phase diagram at a defect line of strength $J \sim 1/\tilde{h}$ in the critical AT model. Left panel: symmetric defect, right panel: asymmetric defect for the σ and τ spins. The RG flow is different for different signs of the bulk four-spin coupling ϵ . For $\epsilon > 0$, the flow is towards the ordinary interface fixed point (OI) when $J < 1$ and the extraordinary interface fixed point (EI) when $J > 1$, both for symmetric and asymmetric defects. When $\epsilon < 0$, the flow is to the bulk fixed point for a symmetric defect. For asymmetric defect the RG flow is different for σ and τ spins.

in the energetically favorable state one set of spins is disordered (being in the OI fixed point) and the other set of spins is ordered (EI fixed point). This is the situation we have found numerically and which is shown in the phase diagram in the right panel of Fig.4.

The field-theoretical results about the spin-spin correlation function at the defect line suggest a different RG phase diagram[16]. According to this theory, which expected to hold for positive Boltzmann-weights ($\epsilon > 0$) the coupling term is an irrelevant perturbation and the critical behavior at the defect is the same as for the decoupled systems. Our numerical results are in contradiction with this scenario. In this respect we mention that in the asymmetric defect problem two potentially marginal operators are involved. One is the product of the energy-densities in the AT model and the second is the local energy-density (line defect) in the Ising model with σ spins. The interplay of these two perturbations at the critical point could result in the phase diagram in Fig.4 which is consistent with our numerical calculations.

Acknowledgments

This work has been supported by Kuwait University Research Grant No. SP01/10. We thank L. Turban for useful discussions.

-
- [1] F. Iglói, I. Peschel, and L. Turban, *Advances in Physics* **42**, 683 (1993).
 - [2] T. W. Burkhardt, in *Proceedings of the XXth Winter School, Karpacz, Poland, 1984*, Lecture Notes in Physics, edited by A. Pekalski and J. Sznajd (Springer, Berlin, 1984), Vol. 206, p. 169.
 - [3] T. W. Burkhardt and E. Eisenriegler, *Phys. Rev. B* **24**, 1236 (1981).
 - [4] H. W. Diehl, S. Dietrich and E. Eisenriegler, *Phys. Rev. B* **27**, 2937 (1983).
 - [5] E. Eisenriegler and T. W. Burkhardt, *Phys. Rev. B* **25**, 3283 (1982).
 - [6] K. Binder, in *Phase Transitions and Critical Phenomena*, edited by C. Domb and J. L. Lebowitz (Academic, London, 1983), Vol. 8, p. 1.
 - [7] H. W. Diehl in *Phase Transitions and Critical Phenomena*, edited by C. Domb and J. L. Lebowitz (Academic Press, London, 1986), Vol. 10, p. 75.
 - [8] M. Pleimling, *J. Phys. A* **37**, R79 (2004).
 - [9] M. P. Nightingale and H. W. J. Blöte, *J. Phys. A* **15**, L33 (1982).
 - [10] F. Iglói and L. Turban, *Phys. Rev. B* **47**, 3404 (1993).
 - [11] Á. Bagaméry, L. Turban, and F. Iglói, *Phys. Rev. B* **73**, 144419 (2006).
 - [12] P. Lajkó, L. Turban, and F. Iglói, *Phys. Rev. B* **76**, 224423 (2007).
 - [13] R. Z. Bariev, *Zh. Eksp. Teor. Fiz.* **77**, 1217 (1979) [*Sov. Phys.-JETP* **50**, 613 (1979)]
 - [14] B. M. McCoy and J. H. H. Perk, *Phys. Rev. Lett.* **44**, 840 (1980).
 - [15] C. Naon and M. Trobo, *J. Stat. Mech.* P02021 (2011).
 - [16] C. Naon, *Phys. Rev. E* **79**, 051112 (2009).
 - [17] J. Ashkin and E. Teller, *Phys. Rev.* **64**, 178 (1943).
 - [18] R. Baxter, *Phys. Rev. Lett.* **26**, 832 (1971).
 - [19] C. Fan, *Phys. Lett.* **39A**, 136 (1972).
 - [20] R. J. Baxter, *Exactly Solved Models in Statistical Mechanics*, (Academic, London, 1982).
 - [21] M. Kohmoto, M. den Nijs, and L.P. Kadanoff, *Phys. Rev. B* **24**, 5229 (1981).
 - [22] F. Iglói and J. Sólyom, *J. Phys. A* **17**, 1531 (1984).
 - [23] For recent reviews about the DMRG method, see: U. Schollwöck, *Rev. Mod. Phys.* **77**, 259 (2005); K. Hallberg, *Advances in Physics* **55**, 477 (2006); U. Schollwöck, *Annals of Physics* **326**, 96 (2011).
 - [24] J. L. Cardy, in *Phase Transitions and Critical Phenomena*, edited by C. Domb and J. L. Lebowitz (Academic, London, 1987), Vol. 11.
 - [25] B. Nienhuis, in *Phase Transitions and Critical Phenomena*, edited by C. Domb and J. L. Lebowitz (Academic, London, 1987), Vol. 11.
 - [26] G. von Gehlen and V. Rittenberg, *J. Phys. A* **20**, 227 (1987).
 - [27] E. Carlon, F. Iglói, W. Selke and F. Szalma, *J. Stat. Phys.* **96**, 531 (1999)